The Evolution of Community Bank Interconnectedness

Giorgi Nikolaishvili*
University of Oregon

January 2023
(Preliminary & Incomplete)

Abstract

I find that the community banking sector in the United States has become more interconnected since the global financial crisis, which implies greater exposure to systemic risk and increased vulnerability in future financial crises. I estimate a hierarchical dynamic factor model using a Bayesian approach to extract posterior distributions of national, regional, and state-level latent drivers of quarterly fluctuations in state-average community bank return-on-equity for all 50 US states. The resulting estimates show evidence of both considerable national comovement and state-specific idiosyncrasy with no signs of significant regional comovement. Furthermore, the results show a decrease in the intensity of idiosyncratic dynamics of state-level community bank profitability since the crisis, along with an increase in national comovement across most states.

JEL Classifications: C38; G01; G21

Keywords: Community banking; dynamic factor modeling; financial crisis

*I thank Jeremy Piger for his many helpful comments and suggestions throughout the writing of this paper. I am also grateful to David Evans and participants at the University of Oregon Macro Group for their feedback. All errors are my own. Email: gnikolai@uoregon.edu.

1 Introduction

The total market share of community banks in the greater US banking sector has experienced a steady decline over the past few decades. Despite the gradual drop in size, mainly due to consolidation, community banks support economic growth and stability through the provision of loans to small local borrowers. Historically, community banks have played a significant role in providing services to rural communities – as of June, 2020, community bank branches held approximately 2/3 of total rural deposits in the US (Hanauer et al., 2021). Furthermore, community banks are major credit providers to agricultural and commercial borrowers in their respective local markets (Lux and Greene, 2015). Community banks have also shown themselves to be reliable credit providers during adverse macroeconomic conditions – most recently during the global financial crisis and the COVID-19 pandemic (Hassan et al., 2022). Lastly, unlike their larger geographically-diversified counterparts, there is reason to believe that community banks' specialization in local market activity may limit the transmission of more global and remote credit shocks (Petach et al., 2021).

After the global financial crisis, the focus of researchers and policymakers on the interconnectedness of large banks formed the consensus that community banks and their potential exposure to common risk factors does not present a threat to the financial system (U.S. Treasury Department, 2017). Policymakers targeted "too-big-to-fail" banks as the cause of the housing bubble, market crash, and the subsequent recession. For this reason, post-crisis regulatory reforms, most notably the Dodd-Frank Wall Street Reform and Consumer Protection Act, largely aimed at constraining the involvement of large banks in risky activities. A key focus of these regulatory changes was the alleviation of the extent of interconnectedness and exposure to systemic risk among large banks (Yellen, 2013). A further revelation of the belief that community banks cannot contribute to systemic risk manifested in the exemption of community bank holding companies from certain regulatory capital requirements. In fact, post-crisis sentiment on the supposed adverse effects of Dodd-Frank on the competitiveness of community banks led to the de-regulation of the community banking sector through the Economic Growth, Regulatory Relief, and Consumer Protection Act (EGRRCPA), passed by Congress in 2018 (Kress and Turk, 2020). I aim to fill a gap in the academic and policy literature by investigating the notion that community banks lack exposure to systemic risk.

In this study I find that state-level community bank performance in the United States has been co-moving less idiosyncratically at the state level and more similarly at the national level since the occurrence of the global financial crisis, relative to the pre-crisis era. This development implies a fundamental and arguably undesirable deviation of the community banking sector from its traditional role in the US financial system. Stronger national comovement of state-level community bank performance is consistent with greater national interconnectedness of community banks, as well as a potential increase in common exposure to macrofinancial shocks.[1] In other words, the relative decrease in (state-level) idiosyncrasy may result in a future financial crisis having a more intensely adverse and uniform effect on the community banking sector. This is precisely the small bank equivalent to the concept of "too-big-to-fail", aptly named "too-many-to-fail" – an increase in the exposure of many small banks to the same sources of risk may lead to their mass failure in the event of a large adverse shock, with devastating effects on the financial system. This effectively brings community banks closer to large banks with respect to their risk profiles, thus shrinking the risk diversification opportunity choice set of depositors. These changes may be a result of either the various post-crisis regulatory policy changes in the banking sector, a push toward more nationally and/or globally diversified asset portfolio allocations by the community banks themselves, or perhaps some deeper structural change caused directly by the financial crisis.

My findings contribute to our understanding of the manner in which the US community banking sector has been evolving in recent decades, as well as the trajectory it may adopt for the near future. Once again, I identify an increase in the extent to which community bank performance co-moves across the country, along with a decrease in the extent of state-level idiosyncrasy. I obtain this insight by capturing dynamic and cross-sectional co-variation across a balanced panel of state-average community bank return-on-equity (ROE) series using a hierarchical dynamic factor model (HDFM), estimated using a Bayesian approach. A careful analysis of national and regional variance decompositions of the country- and region-level factors across pre-crisis, intra-crisis, and post-crisis subsamples shows a near-uniform decrease in state idiosyncrasy for both intra- and post-crisis subsamples relative to the pre-crisis subsample, and a near-uniform increase in national comovement for both intra- and post-crisis subsamples relative to the pre-crisis subsample.

The remainder of this paper is structured as follows: Section 2 is a review of the existing literature on systemic risk in the banking sector, community banks, and HDFMs; Section 3 describes the data and the structure of the HDFM; Section 4 presents and analyzes the results; Section 5 provides an interpretation of the results along with a discussion of their implications.

[1] Stronger national comovement may also be evidence of a persistent post-crisis increase in the magnitude of macrofinancial shocks. Despite this likely being true for the intra-crisis period, existing indicators of financial market volatility, such as the Chicago Board Options Exchange Volatility Index (CBOE VIX), point to a reversion to pre-crisis shock magnitudes after the end of the crisis.

2 Related Literature

In this section I review the existing literature associated with the domain and methodology of this study. I partition the literature into groups of studies on the following topics: (1) the causes and effects of the interconnectedness of banks, as well as the nature of systemic risk associated with such interconnectedness; (2) the nature and evolution of the US community banking sector; (3) the application of hierarchical dynamic factor modeling in macroeconomics. This study contributes to all of the above strands of literature in the analysis of community bank interconnectedness using hierarchical dynamic factor modeling.

2.1 Bank Interconnectedness and Systemic Risk

The level of bank interconnectedness can be used to gauge the presence of systemic risk in the banking system. Systemic risk may arise due to exposure to common factors – for example, Caccioli et al. (2014) find that overlapping portfolios of financial institutions may lead to contagion. For a comprehensive coverage of literature on systemic risk, some of which touches on the manifestation of systemic risk in banking systems, refer to Jackson and Pernoud (2021). Interdependencies among financial institutions may also amplify and create channels for local shocks to propagate within the entire financial system (Eisenberg and Noe, 2001). For example, Elsadek Mahmoudi (2021) shows how a local credit shock induced by hurricane Katrina has affected real and credit markets in distant regions in the United States. More notably, Acemoglu et al. (2015) generalizes the results of Eisenberg and Noe (2001) to find that while a densely connected network of financial institutions likely supports financial stability, it may also lead to more severe propagation of large shocks. Similarly, Gai et al. (2011) find that greater complexity and concentration in a financial network make such systems more fragile to shocks.

I contribute to this line of literature by identifying the dynamic interconnectedness of a large set of small banks across multiple geographical levels using a reduced form approach with minimal structural assumptions. Dynamic interconnectedness is measured by observing the extent of dynamic comovement among a set of bank-specific or aggregated financial bank data using variance decompositions of a given set of series – the greater the variance contribution of a dynamic factor at a certain geographical level (country, region, state, etc.), then the greater the dynamic comovement, and therefore the greater the interconnectedness among banks at that geographical level. Relative to existing methods of measuring bank interconnectedness, my approach is arguably more flexible and intuitive due to its atheoretical dimension-reducing nature, while also capturing complex dynamic relationships with clear policy implications. Kapinos et al. (2020) develop a measure of the dynamic interlinkages among a small set of bank holding corporations using a similar approach. They use a dynamic factor model with time-varying parameters and stochastic volatility in the style of Del Negro and Otrok (2011) to decompose a balanced panel dataset of the return-on-assets (ROA) and net chargeoffs (NCO) series of 86 US bank holding companies as a linear combination of a common factor and a unit-specific idiosyncratic disturbance terms. Unlike this study, Kapinos et al. (2020) do not account for potential geographical factor hierarchies.

2.2 Community Banking

Peer-reviewed literature on community banking is presently quite scarce. However, a few works such as Yeager (2004), Emmons et al. (2004), Meslier et al. (2016), Estes (2014), and Swanson and Zanzalari (2021) pursue a similar interest of identifying the contributions and importance of risk diversification for community banks. Yeager (2004) explores whether decrease in the number of community banks in the US is a result of their preference for geographic diversification as a way of gaining more robustness in the face of local economic shocks. The study finds that community banks withstand local economic shocks well, and therefore geographic diversification must not play a part in driving consolidation in the US community banking sector. Emmons et al. (2004) find that risk-adjusted return for community banks increases along with their size, which they interpret as evidence of idiosyncratic risk dominating local market risk in the community banking sector. Meslier et al. (2016) find that for small banks, intrastate diversification increases risk-adjusted returns and decreases default risk. Estes (2014) studies the relationship between community bank performance and a variety of portfolio diversification strategies, and finds that diversification may improve risk-adjusted performance. Swanson and Zanzalari (2021) explore the question of whether local labor markets impact bank profitability. Their study finds that an increase in the local market unemployment rate decreases bank profitability, with the additional (counter-intuitive) insight that the impact of local market conditions on profitability is less severe for small banks relative to large banks.

The remaining literature on community banks studies evolution of various characteristics of, and causes of heterogeneity within, the community banking sector. DePrince et al. (2011) explore the determinants of interstate heterogeneity in community bank profitability, and find significant relationships between variation in state-average return on assets (ROA) and each state's economic, demographic, and market structure characteristics. Feng and Zhang (2012) find that relative to large banks, community banks had experienced significantly lower productivity growth and lower levels of returns to scale over the 1997-2006 period. Fang and Yeager (2020) study the ability of community banks to withstand severe and prolonged periods of credit losses. They find that community banks had become less sensitive to such adverse circumstances after the global financial crisis relative to the pre-crisis era. Rice and Rose (2016) find that community banks exposed to the government-sponsored enterprises (GSEs) Fannie Mae and Freddie Mac saw slower loan growth post-crisis than their unexposed peers.

The majority of existing community bank studies focus on the effects of various bank-specific properties and exogenous macroeconomics events on community bank performance at the micro level. Instead, my study explores the evolution of the relationship between community banks across the country with respect to their performance, while implicitly accounting for bank-specific and macroeconomic events.

2.3 Hierarchical Dynamic Factor Models

Dynamic factor models (DFMs) have been in use as a method of atheoretically capturing business cycle dynamics since Sargent and Sims (1977). DFMs allow to capture the comovement of a large set of series by modeling the underlying data-generating process (DGP) as being driven by a vector of common autoregressive latent factors. Refer to Doz and Fuleky (2020) for an overview of fundamental DFM estimation approaches, and to Stock and Watson (2016) for an excellent survey of the use of DFMs in macroeconomics. A discussion of DFM identification is presented in Bai and Wang (2012). Multi-level/hierarchical dynamic factor models (HDFMs) are a type of DFM that partitions series into groups across multiple levels, and assigns a latent dynamic factor to each group. Moench et al. (2013) presents a general description of an HDFM. Kose et al. (2003) applies an HDFM to a large panel of country-level data to estimate world, region, and country-specific factors representing business cycle fluctuations. Kose et al. (2008) similary applies an HDFM to G-7 country series to estimate common and country-specific business cycle factors.

3 Model

In the following two subsections I describe the data used in the study, along with the specification of the HDFM applied to the data, respectively. For details on how the HDFM is estimated, refer to Appendix A.

3.1 Data

The dataset used in this study is a balanced panel of 50 series, with each representing the state-average community bank return on equity (ROE) of a state in the United States. Each series has 115 observations, running from Q4 of 1992 up to Q2 of 2021. The series are constructed using raw bank-level quarterly call report data provided publicly by the Statistics on Depository Institutions (SDI) database maintained by the Federal Deposit Insurance Corporation (FDIC). The following procedure is carried out to generate the final state-level dataset used in this study, in the given order:

1. Select net income and equity variables for each quarter;
2. Generate a new ROE variable defined as
$$\text{ROE} = \frac{\text{Net income}}{\text{Equity}};$$
3. Filter for community banks (SDI database contains a binary categorization variable that classifies each observation as belonging to a community bank when true);
4. Match the community banks by each quarter with corresponding geographical variables – particularly, each community bank must be assigned to a US state and the corresponding FDIC supervisory region under which the given state falls (the following 6 regional FDIC offices oversee the entirety of the United States: Atlanta, Chicago, Dallas, Kansas City, New York, San Francisco);
5. Group ROE by state for each quarter, and compute state-average ROE;
6. Combine quarterly data into a single dataset containing a balanced panel of 50 state-average community bank ROE series;
7. Seasonally adjust each series with seasonal-trend (STL) decomposition using locally estimated scatter plot smoothing (LOESS) (Cleveland et al., 1990).[2] Refer to Fig. 1 for randomly-selected timeplots comparing raw and seasonally-adjusted state-average ROE series.

[2]Effectively, the average deviation from the full-sample average of the quarter corresponding to each observation is subtracted from the observed value.

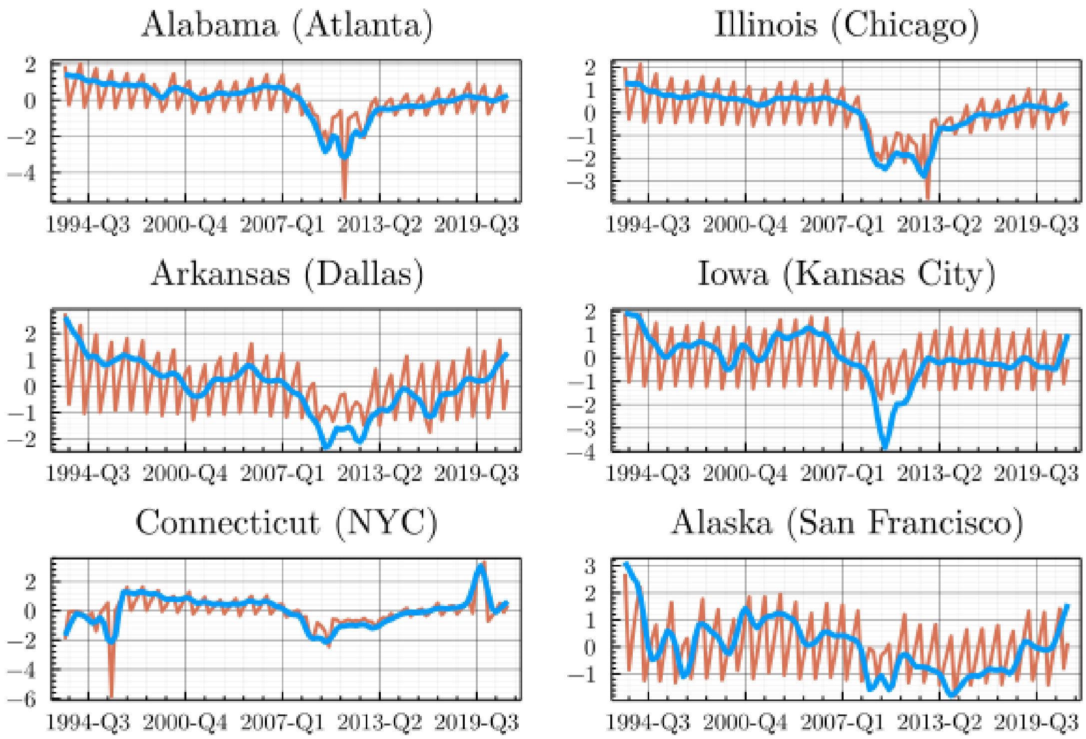

Figure 1: This graph presents a timeplot of normalized level state-average ROE series for one state in each FDIC supervisory region (in orange), along with its seasonally adjusted equivalent (in blue). The supervisory region corresponding to each state is written in parentheses next to their respective subplot labels.

Note that the number of community banks implicitly contained in the final dataset does not stay constant over time – some banks do not survive over the course of the entire sample period, while others are established after the initial sample period. Therefore, the variation in the finalized series is partially driven by young, failing, and ultimately-consolidated community banks. Alternatively, I could have constructed the final state-level dataset by initially filtering out such banks from the raw bank-level data, but this would have yielded a biased picture of actual performance of the community banking of each state at each given point in time. Refer to Fig. 2 for timeplots of the total number of US community banks, and the number of community banks by state over the sample period.

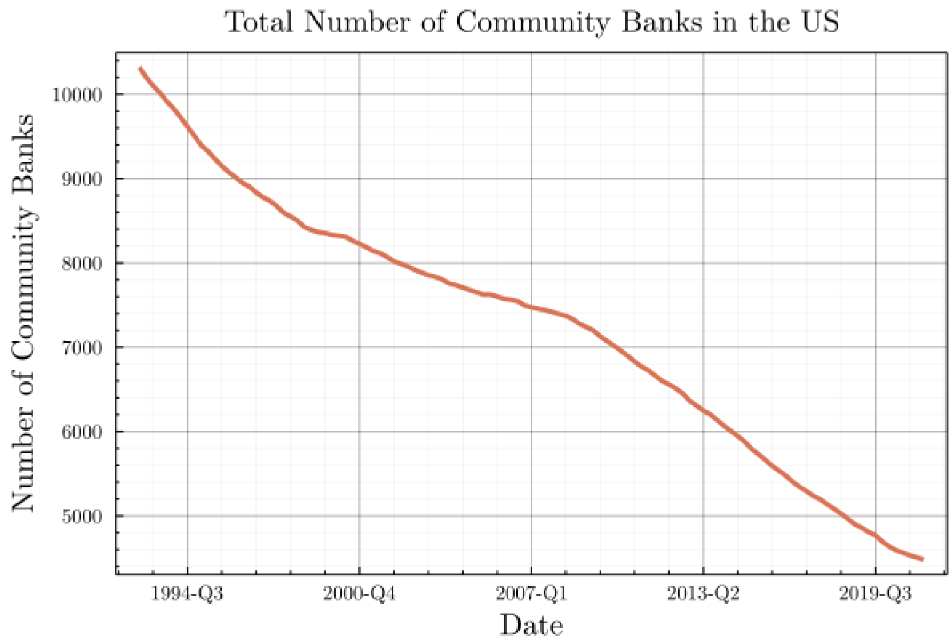

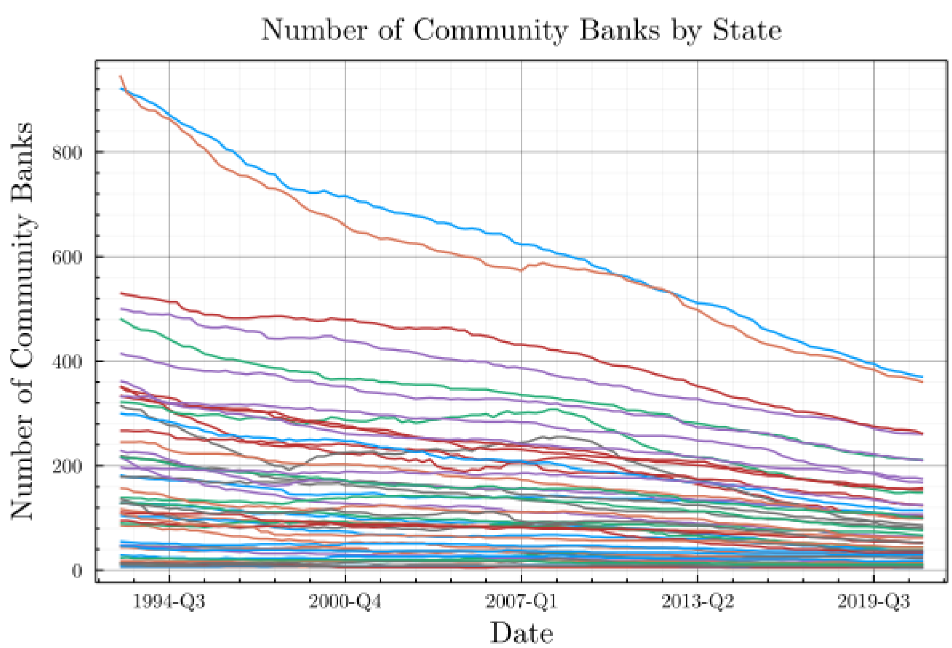

Figure 2: The top plot in this figure represents the total number of community banks in the US over the full sample period. The bottom plot represents the total number of community banks by state over time (each series represents one of 50 US states).

3.2 HDFM

The i-th series in the dataset, expressed as y_i for $i \in \{1, \ldots, I\}$ with $I = 50$, is treated as being generated by an affine combination of a country-wide factor, f^{US}, and a corresponding region-wide factor, f^{r_i}, in the following manner:

$$y_{it} = \beta_{0i} + \beta_{1i} f_t^{US} + \beta_{2i} f_t^{r_i} + \varepsilon_{it}\,, \tag{1}$$

where $\beta^i = (\beta_{0i}, \beta_{1i}, \beta_{2i})$ are coefficient hyperparameters, and ε_i is the idiosyncratic disturbance process specific to the i-th state. Notice that the country-wide factor, f^{US}, applies to all series. There exist a total of $R = 6$ FDIC supervisory regions, f^r, such that state i belongs to only one corresponding region $r_i \in \{1, \ldots, R\}$.

All latent factors and idiosyncratic disturbance terms are modeled as following autoregressive processes. The country factor may be expressed as the following order-p autoregressive process:

$$f_t^{US} = \psi_1^{US} f_{t-1}^{US} + \ldots + \psi_p^{US} f_{t-p}^{US} + v_t^{US}\,, \tag{2}$$

where $\psi^{US} = (\psi_1^{US}, \ldots, \psi_p^{US})$ are lag coefficient hyperparameters, and $v_t^{US} \in i.i.d.N(0, \sigma_{US}^2)$ is an innovation term. The r-ith regional factor may similarly be expressed as the following order-q autoregressive process:

$$f_t^r = \psi_1^r f_{t-1}^r + \ldots + \psi_q^r f_{t-q}^r + v_t^r\,, \tag{3}$$

where $\psi^r = (\psi_1^r, \ldots, \psi_q^r)$ are lag coefficient hyperparameters, and $v_t^r \in i.i.d.N(0, \sigma_r^2)$ is an innovation term. Lastly, the state-specific idiosyncratic disturbances may also be expressed as the following order-k autoregressive process:

$$\varepsilon_{it} = \phi_1^i \varepsilon_{it-1} + \ldots + \phi_k^i \varepsilon_{it-k} + u_t^i\,, \tag{4}$$

where $\phi^i = (\phi_1^i, \ldots, \phi_k^i)$ are lag coefficient hyperparameters, and $u_t^i \in i.i.d.N(0, \sigma_i^2)$ is an innovation term.

The above-specified model has the following restrictions. Firstly, it is assumed that $\sigma_{US}^2 = \sigma_r^2 = 1$. This restriction allows us to simultaneously identify the magnitude of the factors and their β coefficients in Eq. (1), both of which are otherwise unidentified. Secondly, it is assumed that $\beta_{11} > 0$, which enforces a positive relationship between the country factor and the first series in dataset. This assumption is necessary to identify the direction of f^{US}, which may otherwise be mirrored along with the β_{1i} coefficients to yield an identical unconditional distribution. In addition, it is assumed that $\beta_{2i} > 0$ for the first i in each level-2 state region groups for the same reason of identifying the direction of the regional factors. Lastly, it is assumed that $p = q = k = 3$ – in other words, all latent factors and idiosyncratic disturbance processes have the same lag order of 3.[3] This completes the specification of the HDFM assumed to be generating the state-average ROE series.

To be able to apply the Kim-Nelson estimator, we must express the given HDFM in state-space form. Let $\beta_0 = \begin{bmatrix} \beta_{01} & \beta_{02} & \dots & \beta_{0I} \end{bmatrix}'$ be an $I \times 1$ matrix containing the intercept terms of all series in the dataset. Also, let $\beta_1 = \begin{bmatrix} \beta_{11} & \beta_{12} & \dots & \beta_{1I} \end{bmatrix}'$ be an $I \times 1$ matrix containing the national factor loadings of all series in the dataset. Let $\mathbf{R}$ be an $I \times R$ matrix containing the regional factor loadings of all series in the dataset, such that $\mathbf{R}_{ij} = 0$ if the j-th regional factor does not correspond to state i, and $\mathbf{R}_{ij} = \beta_{i2}$ otherwise. Lastly, we define the vector $S_t \equiv \begin{bmatrix} f_t^{US} & f_t^1 & \dots & f_t^R & \varepsilon_{1t} & \dots & \varepsilon_{It} \end{bmatrix}$ of length $L = 1 + R + I$. Given these objects, we may express the measurement equation of the state-space form of the HDFM as

$$\begin{bmatrix} y_{1t} \\ y_{2t} \\ \vdots \\ y_{It} \end{bmatrix} = \begin{bmatrix} \beta_0 & \beta_1 & \mathbf{R} & I & \mathbf{0}_{(1+Lp)\times(1+Lp)} \end{bmatrix} \begin{bmatrix} 1 \\ S_t \\ S_{t-1} \\ \vdots \\ S_{t-p} \end{bmatrix}. \tag{5}$$

If we denote the state vector as β_t, then we may express the state equation as

$$\beta_t = F\beta_{t-1} + w_t\,, \tag{6}$$

where F is a companion matrix and w_t contains i.i.d. disturbance terms. The second moment matrix of w_t may be expressed as the following $(1+Lp)\times(1+Lp)$ matrix:

$$E(w_t w_t') = Q = \begin{bmatrix} 0 & 0 & 0 & \dots & 0 \\ \vdots & I_{1+R} & 0 & \vdots & \vdots \\ \vdots & \mathbf{0}_{(1+R)\times(1+R)} & \Sigma & \vdots & \vdots \\ \vdots & \dots & \mathbf{0}_{((L-1)p)\times((L-1)p)} & \vdots & \vdots \end{bmatrix}, \tag{7}$$

[3]The lag specification of the model is chosen to be parsimonious, while also including enough parameters to account for complex dynamics in quarterly data. While it is possible to test for the optimal number of lags for each of the latent processes using model selection criteria, I have chosen to instead default to the standard approach taken in the literature of simply setting the lag orders of each of the latent processes equal to the same reasonable lag order given the frequency of the data. As examples of this, refer to Kose et al. (2003), Kose et al. (2008), and other HDFM studies mentioned in the literature review section.

where

$$\Sigma = \begin{bmatrix} \sigma_1^2 & 0 & 0 & \dots & 0 \\ 0 & \sigma_2^2 & 0 & \dots & 0 \\ \vdots & & & \ddots & 0 \\ 0 & & \dots & & \sigma_I^2 \end{bmatrix}. \tag{8}$$

4 Results

In this section I present and describe the quantitative results obtained by estimating the HDFM. I first present the unconditional posterior distributions of all latent dynamic factors. Then I analyze relevant subsample variance decompositions of all observable series with respect to the national factor and idiosyncratic disturbance estimates, and follow up with a similar analysis of the variance contributions of each of the regional factors toward series in their respective regions. I find that the dynamics of the national factor, as evidence by the plot of the unconditional posterior distribution of the national factor, seem to accurately match the major historical developments in the banking sector over the course of the last four decades. And although the regional factor estimates are more difficult to decipher, they too seem to show plausible changes over the same time period. I also show using full-sample variance decompositions that over the entire sample period, regional factors have had very limited contributions to the variation in state-average community bank ROE – the majority of the variation in all series is attributable either to state-specific idiosyncrasy or the national factor. Most importantly, comparisons of variance decompositions of pre-, intra-, and post-global financial crisis subsamples demonstrate that the role of the national factor in driving state-average community bank ROE dynamics has grown since the crisis, while the extent state-specific idiosyncrasy has fallen.

4.1 Factor Estimates

Let us observe the nature of the estimated US national latent dynamic factor. Refer to Fig. 3 for a plot of the posterior distribution of the national factor. Firstly, it is worth noting that the confidence bands around the median of the distribution remain relatively tight throughout the full sample period, which implies that the national factor is estimated with precision. More intuitively, we may say that given the priors and the accuracy of the data, the national factor is unlikely to “look” significantly different from the median of the posterior distribution presented in Fig. 3. Secondly, notice that the path of the median seems to accurately match the 21st century developments in the US banking sector. Starting at around the year 2007 the factor begins to drop, and reaches a trough a few years later, after which it begins to trend upward quite monotonously until the present time.

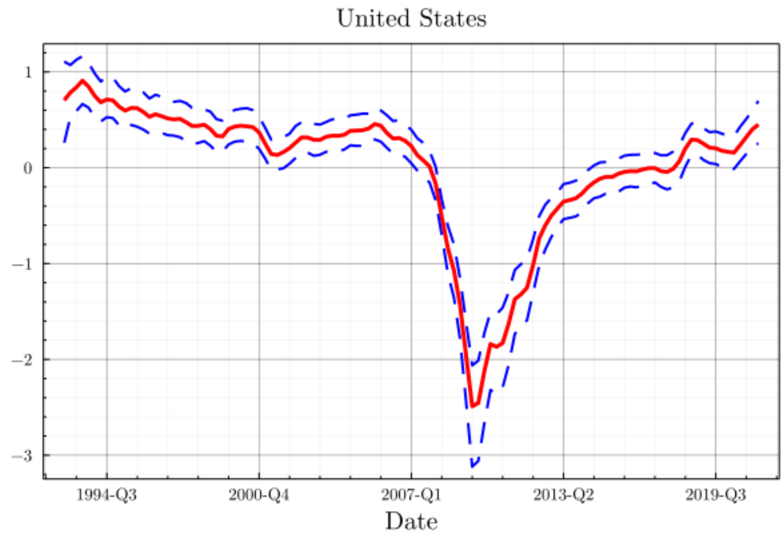

Figure 3: This graph presents a timeplot of the estimated unconditional distribution of the US national latent dynamic factor over the full sample period. The solid red line represents the median of the distribution at each given point in time, while the dashed blue lines represent the 5th and 95th percentiles of the distribution – in other words, the dashed blue lines represent 90% confidence bands around the median.

Furthermore, although the direction of the variation in the latent factors has no clear meaning without knowledge of the directions of the factor loadings, in the given case the interpretation is both clear and consistent since the factor loadings on the national factor with respect to each of the state-average ROE series overwhelmingly have posterior distributions situated convincingly above zero, with *all* of their point estimates and posterior medians being strictly positive. Therefore, a drop in the national factor may directly be interpreted as a nation-wide downward force on the state-average profitability of community banks across the United States. This implies that the behavior of the median of the posterior distribution of the national factor matches the downfall of the US banking sector during the global financial crisis, and the subsequent post-crisis nation-wide recovery. Furthermore, the relatively small pre-crisis variation of the factor above its mean also reflects uneventfulness of the period and the consistently favorable conditions in the banking sector during the Great Moderation.

Unlike the national factor, interpreting the posterior distributions of the regional factors presented in Fig. 7 is more challenging due to the difficulty of identifying FDIC's supervisory region-specific historical events and policy changes in the community banking sector. However, we may still make some stylistic observations regarding the behavior of these posterior distributions. For example, a quality shared by all of the regional factors is the presence of either a sharp "uptick" or "downtick" during the crisis period. Once again, the direction of these changes is not very informative – even with the posterior distributions of these factor loadings it is difficult to make a clear observation about the effects of the factors. Unlike those of the national factor, the regional factor loadings seem to be more inconsistent in their directions across states. Another notable property of the posterior distributions is that they are wider than that of the national factor – this implies less precision, likely caused by the smaller set of data used to estimate the regional factors.

4.2 Full Sample Variance Decompositions

Variance decomposition plots allows us to gauge the extent to which the national and regional factors drive the variation in each of their corresponding state-average ROE series. In Fig. 4, I present a full-sample variance decomposition for all 50 states, from which we may draw a number of conclusion regarding the significance of the roles played by the latent dynamic factors. Firstly, it is apparent that the national factor is a major contributor to the state-average ROE variation for a considerable portion of the states. Secondly, many of the state-average ROE series vary quite idiosyncratically. Thirdly, the regional factors seem to play a minor role in contributing to the variation in all of the states' respective series. Lastly, there is noticeable heterogeneity in the roles of the national factor and state-specific idiosyncrasies across the set of all states – in other words, the majority of the variation in some states may confidently be attributed to the national factor, while the variation in others is overwhelmingly idiosyncratic. Therefore, it is difficult to make qualitative statements regarding the magnitude of the role of the national factor – some states co-move with the rest of the country to significantly lesser degree than others across the full sample period.

A similar graph is presented in Fig. 9, which groups full-sample variance decompositions of each of the state-average ROE series by region. Such grouping allows us to better observe any potential group-specific heterogeneity in full-sample variance contributions by the national and regional factors, as well as state-specific idiosyncrasies. Note that although the HDFM does not explicitly account for such level-2 (regional) variance decomposition dependencies, it also makes no restrictions that may prevent the emergence of such patterns. I make the following observations about the regionally-grouped full-sample variance decompositions presented in Fig. 9: Firstly,

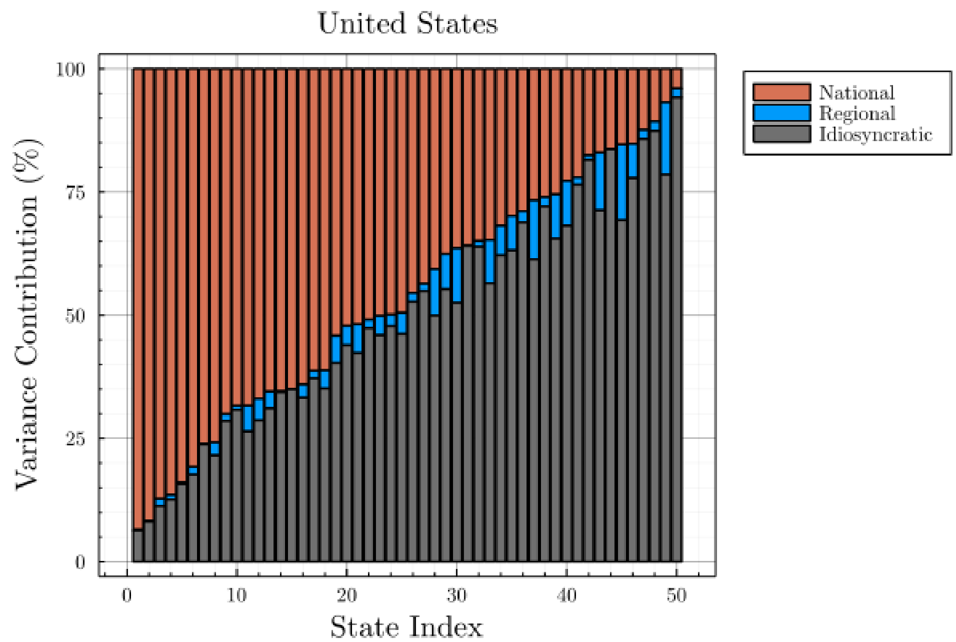

Figure 4: This graph presents the variance decomposition of each of the state-average ROE series in the dataset with respect to the three non-intercept independent variables: (1) the national factor, (2) a corresponding regional factor, and (3) the corresponding state-specific idiosyncratic disturbance process. In other words, the graph shows the percentage of the total variance of each observable series that may be attributed to each of its possible contributing drivers. The state index orders states by their national factor contribution in decreasing order.

there seem to be no clear group-based tendencies in the variation contribution of the national factor, although some regions (e.g. Dallas) seem to have lower average national factor contributions, while others (e.g. Chicago) seem to have consistently higher average national factor contributions. Secondly, the NYC region seems to have consistently grater contributions to its state-average ROE series from its respective regional factor than do the rest. Lastly, there exist no apparent regional group-based patterns in the variation contributions of the state-specific idiosyncratic processes. Therefore, I conclude that there are no notable and/or accountable region-specific tendencies in the full-sample variance decompositions across the six FDIC supervisory regions.

4.3 Subsample Variance Decompositions

Figs. 8-14 in the Appendix present the pre-, intra-, and post-global financial crisis variance contributions of the Atlanta, Chicago, Dallas, Kansas City, New York City, and San Francisco region factors, respectively, to each of their corresponding state-average community bank ROE series. The contribution of the corresponding regional factors for the majority of the states in the Atlanta, Kansas City, and New York City, and San Francisco regions sees a decrease post-crisis relative to the pre-crisis period. The same cannot be said for the rest of the regions, however, which seem to have no other noticeable temporal patterns. Another noteworthy insight from these subsample regional variance decompositions is that the New York City factor seems to influence its corresponding states more strongly throughout the full sample period than any of the other regional factors. Furthermore, it is the only region in which the intra-crisis variance contribution of the regional factor is noticeably greater for most of the related states than its pre- and post-crisis contribution. These properties perhaps reflect the notably strong presence and influence of large financial institutions in the region relative to others.

I present the most striking results of this study in Figs. 5 and 6. I begin by accounting for the results shown in Fig. 5, which compares the contribution of the national factor to the variation in all 50 state-average ROE series across the pre-, intra-, and post-global financial crisis subsamples. The first plot in Fig. 5 compares the pre-crisis and crisis periods, with the former lasting until Q4 of 2006, and the latter starting at Q1 of 2007 and lasting until Q4 of 2009. It is clear that the variance contribution of the national factor saw a significant near-uniform increase during the crisis, relative to the pre-crisis period. Only 2 of the 50 states show a decrease in the variance contribution of the national factor. This result implies that state-average community bank ROE series co-moved more strongly at the national level during the approximate time interval associated with the global financial crisis up until that point since the beginning of the sample period. The second plot in Fig. 5 compares the pre-crisis and post-crisis periods, with the latter starting at Q1 of 2010 and lasting until the end of the sample period at Q2 of 2021. Once again, the variance contribution of the national factor seems to have seen a significant near-uniform increase after the crisis, relative to the pre-crisis period. Only 3 of the 50 states show a decrease in the variance contribution of the national factor after the crisis. This result implies that state-average community bank ROE series co-moved more strongly at the national level since the approximate end of the global financial crisis period than it did before its approximate beginning. In summary, the results presented in Fig. 5 demonstrate that the extent of national comovement among the state-average community bank ROEs has increased nearly uniformly since the start of the global financial crisis.

Next I describe the results shown in Fig. 6, which compares the contribution of the state-specific idiosyncratic disturbance processes to the variation in all 50 of their corresponding state-average ROE series across the pre-, intra-, and post-global financial crisis subsamples. The first plot in Fig. 6 compares the pre-crisis and crisis periods. It is apparent that the variance contribution of the state-specific idiosyncratic processes saw a significant near-uniform decrease during the crisis, relative to the pre-crisis period. Only 4 of the 50 states show an increase in state-specific idiosyncrasy. This result implies that state-average community bank ROE series varied more idiosyncratically during the global financial crisis up until its occurrence since the beginning of the sample period. The second plot in Fig. 6 compares the pre-crisis and post-crisis periods. Once again, the variance contribution of the state-specific idiosyncratic processes saw a significant near-uniform decrease after the end of the crisis, relative to the pre-crisis period. Only 5 of the 50 states show a increase in state-specific idiosyncrasy. This result implies that state-average community bank ROE series varied more idiosyncratically since the end of the global financial crisis period than it did before its beginning. In summary, the results presented in Fig. 6 demonstrate that the extent of state-specific dynamic idiosyncrasy among the state-average community bank ROEs has decreased nearly uniformly since the start of the global financial crisis. Notice that this result does not deliver the same information as that given by Fig. 5, but rather complements it – the latter does not consider the potential changes in regional comovement, while the former accounts for changes in the sum of national and regional comovement.

In Fig. 3 it is apparent that much of the variation in the national factor is contained in the post-crisis subsample is contained between the very beginning of said subsample and Q1 of 2013. This may leave the reader questioning whether the shown increase in the variance contribution of the national factor is attributable solely to this period of high national factor volatility, after which it returns to its pre-crisis contribution level. However, it is also true that the state-average ROE series generally show the same type of behavior – most of them exhibit a considerable drop during the crisis period, followed by a slow convergence back to their pre-crisis levels. The significant determinant of the source of the post-crisis increase in variance contribution is the *relative* behaviors of the national factor and the state-average ROE series. To dispel such doubts, I repeat the same variance decomposition analysis by defining the post-crisis period as beginning in Q1 of 2013, and present the results in Figs. 15 and 16 in the Appendix. Although to a lesser extent, this alternative analysis yields the same type of results as the original analysis. This implies that the ratio of post- and pre-crisis average volatility of innovations to the national factor is consistently greater than that of the majority of state-specific disturbance processes. In other words, the increased national comovement of state-average community bank ROEs seems to be a persistent phenomenon.

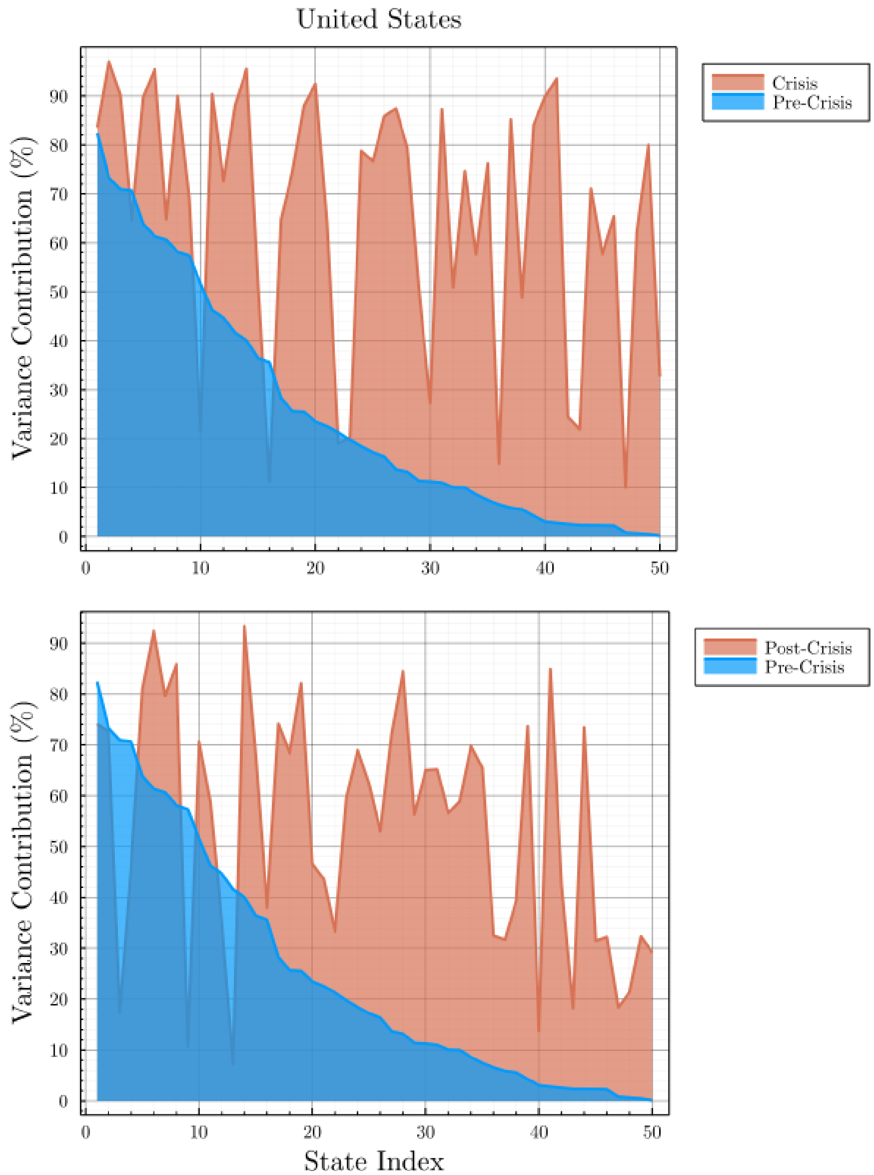

Figure 5: This graph plots the percent variance contribution made by the US national factor toward each of the state-average ROE series in the dataset. The first facet compares the variance contributions made by the national factor during the pre- vs. intra-crisis periods, while the second facet compares that of pre- vs. post-crisis periods. The state index orders states by their pre-crisis national factor contribution in decreasing order.

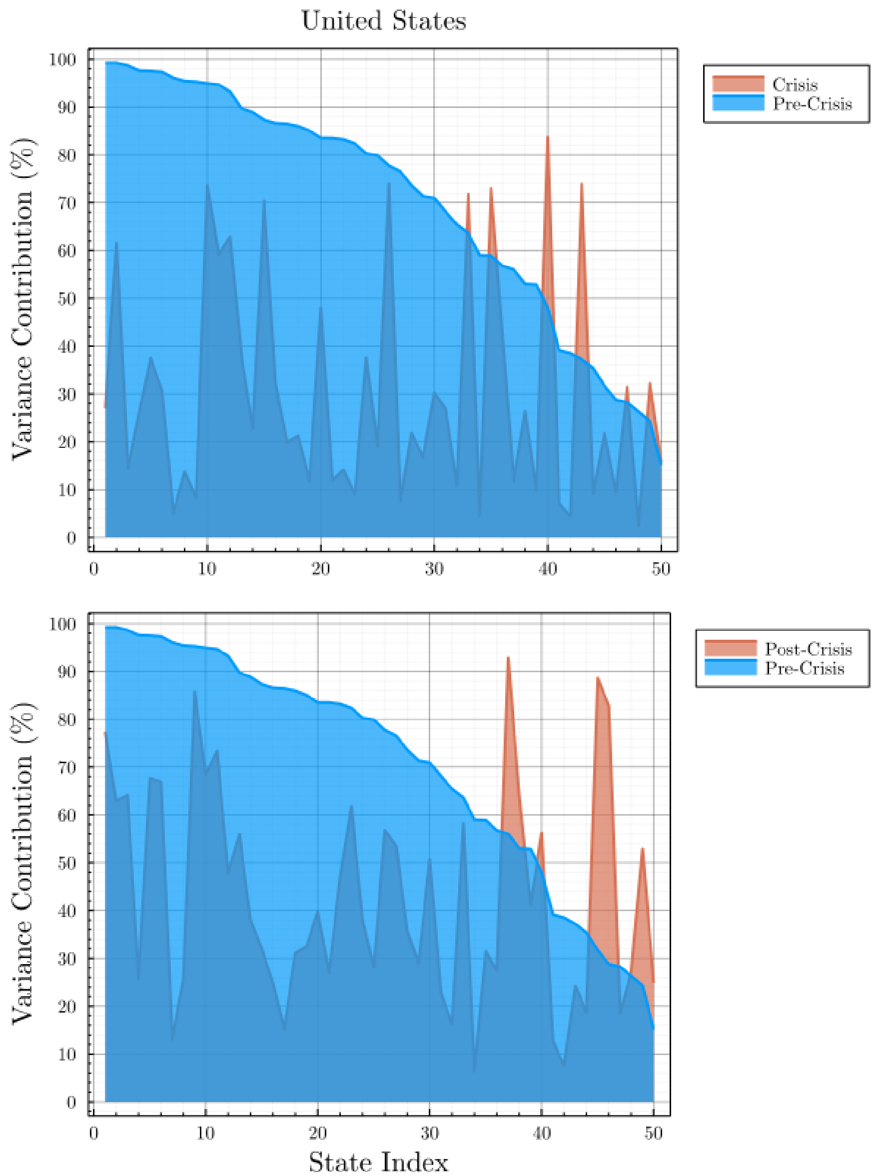

Figure 6: This graph plots the percent variance contribution made toward each of the state-average ROE series in the dataset by their respective idiosyncratic disturbance processes. The first facet compares the variance contributions during the pre- vs. intra-crisis periods, while the second facet compares that of pre- vs. post-crisis periods. The state index orders states by their pre-crisis national factor contribution in decreasing order.

5 Conclusion

In this study I estimate a multi-level / hierarchical dynamic factor model using a balanced panel of 50 state-average community bank return-on-equity series to measure national and region-level comovement, as well as state-specific idiosyncrasy, in community bank profitability at the state level. My analysis shows evidence that (1) there has historically been strong nation-level dynamic comovement in community bank profitability in the United States; (2) there has historically been weak regional comovement in community bank profitability; (3) there has historically been significant state-specific idiosyncratic dynamics to community bank profitability; (4) the extent of national comovement has increased almost uniformly across all states since the global financial crisis, while the extent of state-specific idiosyncrasy has dropped. These empirical findings may be interpreted as showing an increase in the interconnectedness of community banks across the United States since the crisis, which implies an intensification in their exposure to common macrofinancial shocks. The increased interconnectedness leads to greater systemic risk, which in turn increases the likelihood of bank contagion, thus leading to greater negative effects on community banks in the United States in the event of another financial crisis. Based on the historical role of the community banking sector as a source of locally-specialized provider of loans and financial services that also is intended to be less sensitive to adverse macroeconomic shocks (as opposed to large banks), these results seem to shed light on an undesirable trajectory of the evolution of the sector.

An alternative interpretation of the increase in national comovement and decrease in the state-specific idiosyncrasy of community bank profitability, as evidenced by Figs. 5 and 6, respectively, is an increase in the underlying country-level volatility of the banking sector rather than its interconnectedness. I offer a non-rigorous explanation of why this interpretation is likely invalid through a brief discussion in the introductory section of this paper, but I reiterate it here. The underlying volatilities (the magnitudes of structural shocks) of the US banking sector are believed to have increased during the crisis, but reverted back to their normal levels after the end of the crisis (Duffie, 2018; Sykes, 2018; Kim et al., 2020). Furthermore, it is unlikely that the community banking sector underwent a drastically different experience relative to the rest of the banking sector around this time period. For this reason, the increase in comovement is most probably the result of an increase in the structural interconnectedness of community banks across the country. In future works I plan to further explore the validity of this alternative interpretation more rigorously by performing a similar analysis with time-varying parameters (utilizing the approach developed by Del Negro and Otrok (2011)). This method of analysis will allow me to check whether the increased national comovement is the result of a relative increase in the national factor loadings or an increase in its innovation volatility, where the former confirms my original interpretation and the former is evidence of the alternative interpretation.

The increased interconnectedness of the US community banking sector may be the result of a variety of changes that occurred during and immediately after the global financial crisis. Although this study points toward the emergence of this phenomenon, it does little to identify the mechanisms that led to such a development. One likely possibility is the increased interconnectedness being caused by the convergence in the asset portfolio allocations of community banks in an effort to diversify idiosyncratic risk. I believe that testing this hypothesis is a fruitful avenue for future studies, among other reasonable hypotheses as to why the community banking sector in the US has become more interconnected.

References

Acemoglu, B. D., Ozdaglar, A., and Tahbaz-salehi, A. (2015). American Economic Association Systemic Risk and Stability in Financial Networks. *American Economic Review*, 105(v):564–608.

Bai, J. and Wang, P. (2012). Identification and Bayesian Estimation of Dynamic Factor Models. *Journal of Business and Economic Statistics*, 33(2):221–240.

Caccioli, F., Shrestha, M., Moore, C., and Farmer, J. D. (2014). Stability analysis of financial contagion due to overlapping portfolios. *Journal of Banking and Finance*, 46(1):233–245.

Chib, S. (1993). Bayes Regression with Autoregressive Errors. *Journal of Econometrics*, 58:275–294.

Cleveland, R. B., Cleveland, W. S., McRae, J. E., and Terpenning, I. (1990). Stl: A seasonal-trend decomposition procedure based on loess (with discussion). *Journal of Official Statistics*, 6:3–73.

Del Negro, M. and Otrok, C. M. (2011). Dynamic Factor Models with Time-Varying Parameters: Measuring Changes in International Business Cycles.

DePrince, A. E., Ford, W. F., and Morris, P. D. (2011). Some causes of interstate differences in community bank performance. *Journal of Economics and Finance*, 35(1):22–40.

Doz, C. and Fuleky, P. (2020). Dynamic Factor Models. *Advanced Studies in Theoretical and Applied Econometrics*, 52:27–64.

Duffie, D. (2018). Financial Regulatory Reform After the Crisis: An Assessment. *Management Science*, 64(10):4835–4857.

Eisenberg, L. and Noe, T. H. (2001). Sytemic Risk in Financial Systems. *Management Science*, 47(2):236–249.

Elsadek Mahmoudi, S. (2021). The Propagation of Local Credit Shocks: Evidence from Hurricane Katrina. *SSRN Electronic Journal*.

Emmons, W. R., Gilbert, R. A., and Yeager, T. J. (2004). Reducing the risk at small community banks: Is it size or geographic diversification that matters? *Journal of Financial Services Research*, 25(2-3):283–289.

Estes, K. (2014). Diversification and Community Bank Performance. *International Journal of Finance and Banking Studies*, 3(4):1–40.

Fang, C. and Yeager, T. J. (2020). A historical loss approach to community bank stress testing. *Journal of Banking and Finance*, 118:105831.

Feng, G. and Zhang, X. (2012). Productivity and efficiency at large and community banks in the US: A Bayesian true random effects stochastic distance frontier analysis. *Journal of Banking and Finance*, 36(7):1883–1895.

Gai, P., Haldane, A., and Kapadia, S. (2011). Complexity, concentration and contagion. *Journal of Monetary Economics*, 58(5):453–470.

Hanauer, M., Lytle, B., Summers, C., and Ziadeh, S. (2021). Community Banks' Ongoing Role in the U.S. Economy. *The Federal Reserve Bank of Kansas City Economic Review*, pages 37–81.

Hassan, M. K., Karim, M. S., Lawrence, S., and Risfandy, T. (2022). Weathering the COVID-19 storm: The case of community banks. *Research in International Business and Finance*, 60(December 2021):101608.

Jackson, L. E., Kose, M. A., Owyang, M. T., Comovement, P., and Jackson, L. E. (2015). Specification and Estimation of Bayesian Dynamic Factor Models: A Monte Carlo Analysis with an Application to Global House Price Comovement.

Jackson, M. O. and Pernoud, A. (2021). Systemic Risk in Financial Networks: A Survey. *Annual Review of Economics*, 13(December):171–202.

Kapinos, P., Kishor, N. K., and Ma, J. (2020). Dynamic comovement among banks, systemic risk, and the macroeconomy. *Journal of Banking and Finance*.

Kim, C.-J. and Nelson, C. (1999). *State-Space Models with Regime Switching: Classical and Gibbs-Sampling Approaches with Applications*, volume 1. The MIT Press, 1 edition.

Kim, H., Batten, J. A., and Ryu, D. (2020). Financial crisis, bank diversification, and financial stability: OECD countries. *International Review of Economics and Finance*, 65(September 2019):94–104.

Kose, M. A., Otrok, C., and Whiteman, C. H. (2003). International business cycles: World, region, and country-specific factors. *American Economic Review*, 93(4):1216–1239.

Kose, M. A., Otrok, C., and Whiteman, C. H. (2008). Understanding the evolution of world business cycles. *Journal of International Economics*, 75(1):110–130.

Kress, J. C. and Turk, M. C. (2020). Too many to fail: Against community bank deregulation. *Northwestern University Law Review*, 115(3):647–716.

Lux, M. and Greene, R. (2015). The State and Fate of Community Banking. (37).

Meslier, C., Morgan, D. P., Samolyk, K., and Tarazi, A. (2016). The benefits and costs of geographic diversification in banking. *Journal of International Money and Finance*, 69:287–317.

Moench, E., Ng, S., and Potter, S. (2013). Dynamic Hierarchical Factor Models. *The Review of Economics and Statistics*, 95(5):1811–1817.

Petach, L., Weiler, S., and Conroy, T. (2021). It's a wonderful loan: local financial composition, community banks, and economic resilience. *Journal of Banking and Finance*, 126:106077.

Rice, T. and Rose, J. (2016). When good investments go bad: The contraction in community bank lending after the 2008 GSE takeover. *Journal of Financial Intermediation*, 27:68–88.

Sargent, T. J. and Sims, C. A. (1977). Business Cycle Modeling Without Pretending to Have Too Much A Priori Economic Theory.

Stock, J. H. and Watson, M. W. (2016). *Dynamic Factor Models, Factor-Augmented Vector Autoregressions, and Structural Vector Autoregressions in Macroeconomics*, volume 2. Elsevier B.V., 1 edition.

Swanson, A. and Zanzalari, D. (2021). Do local labor market conditions impact bank profitability? *Review of Financial Economics*, 39(3):314–333.

Sykes, J. B. (2018). *Regulatory reform 10 years after the financial crisis: Systemic risk regulation of non-bank financial institutions*.

U.S. Treasury Department (2017). A Financial System That Creates Economic Opportunities: Banks and Credit Unions. (Executive Order 13772):1–137.

Yeager, T. J. (2004). The demise of community banks? Local economic shocks are not to blame. *Journal of Banking and Finance*, 28(9):2135–2153.

Yellen, J. L. (2013). Interconnectedness and Systemic Risk: Lessons from the Financial Crisis and Policy Implications Remarks.

Appendices

A Estimation Methodology

The HDFM hyperparameters and latent factors are estimated by iteratively drawing samples from their respective conditional posterior distributions using the following sampling procedure:

1. Initialize the latent factors, $(f^{US})^0$ and $(f^r)^0$ for $r = 1,\dots,R$, by computing them using the PCA approach discussed in Jackson et al. (2015), and initialize hyperparameters by setting all regression coefficients to 0 and innovation variances to 1;
2. Draw β^j from $p(\beta\,|\,\phi^{j-1},(\sigma^2)^{j-1},\text{factors}^{j-1})$ for each i-th observable series;
3. Draw ϕ^j from $p(\phi\,|\,\beta^j,(\sigma^2)^{j-1},\text{factors}^{j-1})$ for each i-th observable series;
4. Draw $(\sigma^2)^j$ from $p(\sigma^2\,|\,\beta^j,\phi^j,\text{factors}^{j-1})$ for each i-th observable series;
5. Draw $(f^{US})^j$ from $p(f^{US}\,|\,\beta^j,\phi^j,(\sigma^2)^j,\text{regional factors}^{j-1})$;
6. Draw $(f^r)^j$ for $r = 1,\dots,R$ from $p(f^{US}\,|\,\beta^j,\phi^j,(\sigma^2)^j,(f^{US})^j)$.
7. Repeat until $j = J = 5,000$, and discard the first $M = 1,000$ draws to guarantee convergence to a stationary distribution.[4]

Once the above Markov Chain Monte Carlo (MCMC) procedure is executed, the outcome will yield large samples of the unconditional posterior distributions of model hyperparameters and latent factors that may then be used for inference. The following subsections describe the specifics of how the above-mentioned posterior conditional distributions are constructed and utilized.

A.1 Drawing Hyperparameters

To draw the model hyperparameters, I refer to the methodology developed by Chib (1993), and subsequently applied in a context similar to that of this study by Kim and Nelson (1999). We begin

[4]The choice of sample size and number of burn-in periods is the result of experimenting with the given data and estimator, rather than being a function of rigorous convergence criteria. I have visually observed the convergence properties of all parameter and factor distributions conditional on a set of different initialization conditions, and in all cases the MCMC seems to converge in under 100 periods. Initializing the factors using PCA seems to be most efficient in achieving convergence. Therefore, the choice of 1000 burn-in periods guarantees convergence in the context of this study.

by expressing Eqs. (1) and (4) for any given $i \in \{1,\ldots,I\}$ in stacked form as

$$Y = X\beta + e\,, \tag{9}$$

and

$$e = E\phi + u\,, \tag{10}$$

respectively, such that the columns of X represent an intercept and observations of relevant latent factors. Let $e^* = Y - X\beta$, so that

$$e^* = E^*\phi + u\,. \tag{11}$$

Furthermore, let $Y^* = \Phi(L)Y$ and $X^* = \Phi(L)X$ be quasi-differenced versions of Y and X with respect to the lag polynomial corresponding to that of the autoregressive disturbance process, so that

$$Y^* = X^*\beta + u\,, \tag{12}$$

The constructed objects e^*, E^*, Y^*, and X^* are later used to construct conditional posterior distributions for the model hyperparameters used in the Gibbs sampler.

We begin by constructing the conditional posterior distribution for the β coefficients given the ϕ and σ^2 parameters. The coefficient prior may be expressed as

$$\beta \,|\, \phi, \sigma^2 \sim N(b_0, A_0)\,, \tag{13}$$

where b_0 and A_0 are observed moment priors. It follows that the coefficient posterior may be expressed in the following manner:

$$\beta \,|\, \phi, \sigma^2, Y \sim N(b_1, A_1)\,, \tag{14}$$

where

$$b_1 = \left(A_0^{-1} + \sigma^{-2} X^{*\prime} X^*\right)^{-1} \left(A_0^{-1} b_0 + \sigma^{-2} X^{*\prime} Y^*\right)\,, \tag{15}$$

and

$$A_1 = \left(A_0^{-1} + \sigma^{-2} X^{*\prime} X^*\right)^{-1}\,. \tag{16}$$

At each iteration of the sampler, a new β is drawn for each series $i = 1,\ldots,I$ conditional on previous draws of ϕ and σ^2. If the direction restrictions on the national and regional factor loadings do not satisfy the restrictions imposed on the model (described in Section 3.2), then a given draw is discarded and a new one draw is made. If the direction restrictions are persistently violated, then after 100 such unsatisfactory draws the corresponding factor observations are mirrored around 0, and the above process is repeated until all restrictions are satisfied.

Next, we construct the conditional posterior distribution for ϕ given observations of the β and σ^2 parameters. The idiosyncratic disturbance autoregressive coefficient prior may be expressed as

$$\phi \,|\, \beta, \sigma^2 \sim N(c_0, B_0)\,, \tag{17}$$

where c_0 and B_0 represent our prior beliefs about the first two moments of ϕ. Therefore, the conditional posterior of σ^2 may be expressed in the following manner:

$$\phi \,|\, \beta, \sigma^2, Y \sim N(c_1, B_1)_{I[s(\phi)]}\,, \tag{18}$$

where

$$c_1 = \left(B_0^{-1} + \sigma^{-2} E^{*\prime} E^{*}\right)^{-1} \left(B_0^{-1} c_0 + \sigma^{-2} E^{*\prime} e^{*}\right), \tag{19}$$

and

$$B_1 = \left(B_0^{-1} + \sigma^{-2} E^{*\prime} E^{*}\right)^{-1}. \tag{20}$$

The indicator function $I[s(\phi)]$ keeps only those draws of ϕ that represent covariance-stationary autoregressive processes (roots of the lag polynomial $\phi(L)$ are outside of the unit circle). In the computational implementation of the estimator, ϕ is drawn repeatedly at each iteration of the sampler until desired stationary is achieved.

Lastly, I construct the conditional posterior distribution for σ^2 given observations of the β and ϕ parameters. The innovation variance prior may be expressed as

$$\sigma^2 \,|\, \beta \sim IG\left(\frac{\upsilon_0}{2}, \frac{\delta_0}{2}\right), \tag{21}$$

where υ_0 and δ_0 are observed and represent our beliefs about the distribution of σ^2. The innovation variance conditional posterior distribution corresponding to any given observed series $i \in \{1,\ldots,I\}$

may be expressed in the following manner:

$$\sigma^2 \,|\, \beta, Y \sim IG\left(\frac{\upsilon_1}{2}, \frac{\delta_1}{2}\right), \tag{22}$$

where

$$\upsilon_1 = \upsilon_0 + T \tag{23}$$

and

$$\delta_1 = \delta_0 + (Y^* - X^*\beta)'\,(Y^* - X^*\beta)\,. \tag{24}$$

Since there are no restrictions on the innovation variance parameters, a draw from the above posterior distribution is accepted by default.

A.2 Drawing Level-1 (National) Factor

The estimation of the national factor must be based on the variation in the data without the influence of the regional factors. For this reason, we define z_{it} as being the variation in the i-th observable series attributable only to the national factor and the idiosyncratic disturbance term:

$$z_{it} \equiv y_{it} - \beta_{2i} f_t^{r_i}\,. \tag{25}$$

We are able to partial out the variation in $f_t^{r_i}$ in z_{it} due to the fact that we are conditioning on the regional factors and model hyperparameters to generate the posterior conditional distribution of the national factor, and may therefore treat all else as observed. Once $z_t = (z_{1t}, \ldots, z_{It})$ is computed, we may apply the Kalman filter to it to generate the posterior conditional distribution described by

$$\beta_T \,|\, \widetilde{z}_T \sim N\left(\beta_{T\,|\,T}\,, P_{T\,|\,T}\right) \tag{26}$$

and

$$\beta_t \,|\, \widetilde{z}_t\,, \beta_{t+1} \sim N\left(\beta_{t\,|\,t,\beta_{t+1}}\,, P_{t\,|\,t,\beta_{t+1}}\right)\,, \tag{27}$$

for $t = T-1, T-2, \ldots, 1$, where

$$\beta_{T\,|\,T} = E(\beta_T \,|\, \widetilde{z}_T)\,, \tag{28}$$

$$P_{T\,|\,T} = Cov(\beta_T \,|\, \widetilde{z}_T)\,, \tag{29}$$

$$\beta_{t\,|\,t,\beta_{t+1}} = E(\beta_t \,|\, \widetilde{z}_t, \beta_{t+1} = E(\beta_t \,|\, \beta_{t\,|\,t}, \beta_{t+1})\,, \tag{30}$$

$$P_{t\,|\,t,\beta_{t+1}} = Cov(\beta_t \,|\, \widetilde{z}_t, \beta_{t+1}) = Cov(\beta_t \,|\, \beta_{t\,|\,t}, \beta_{t+1})\,, \tag{31}$$

such that $\tilde{z}_t$ represents the history of z up until period t. Note that the state-space formulation of the model used for the Kalman filter here is a more parsimonious one than, and nested in, the specification given in Section 3.2. More specifically, the given state-space formulation used in the generation of the conditional posterior distribution for the national factor need not contain any regional factor-related components due to the regional factors being treated as observed.

A.3 Drawing Level-2 (Regional) Factors

The regional factors are treated similarly to the national factor. First, we must partial out the variation attributable to the national factor from all of the series corresponding to a given regional factor. Then, we express the subset of the HDFM specifying the random DGP determining the variation in the given series in state-space form, such that all components related to all other series and the national factor are excluded due to being treated as observed. Lastly, we input the Kalman filter-generated objects into the same posterior distribution specified in Section 4.2 in order to make draws of each of the regional factors.

B Figures

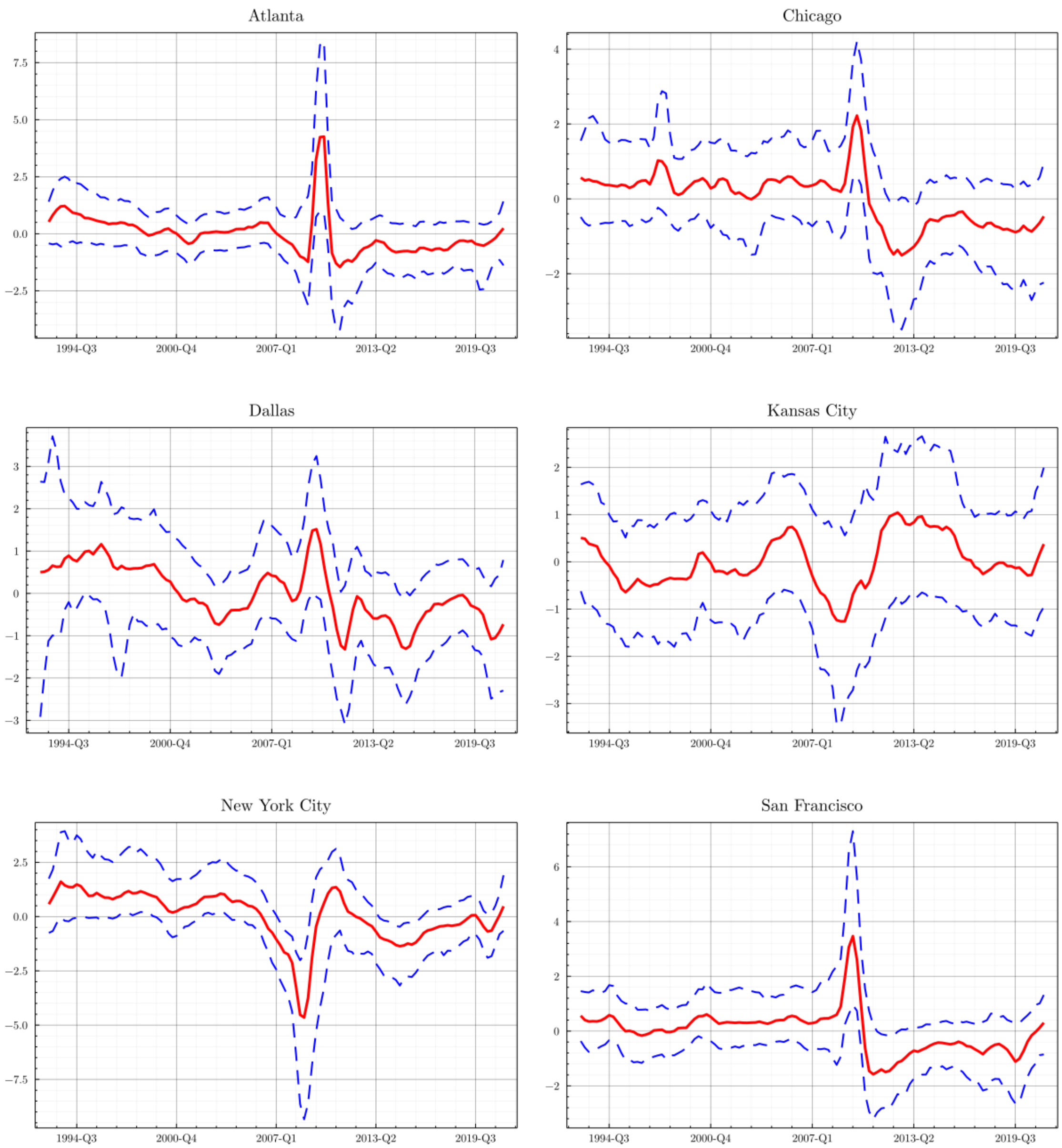

Figure 7: Each of the facets in the given graph presents a timeplot of the estimated unconditional distribution of the corresponding regional latent dynamic factor over the full sample period. The solid red line represents the median of the distribution at each given point in time, while the dashed blue lines represent the 5th and 95th percentiles of the distribution – in other words, the dashed blue lines represent 90% confidence bands around the median.

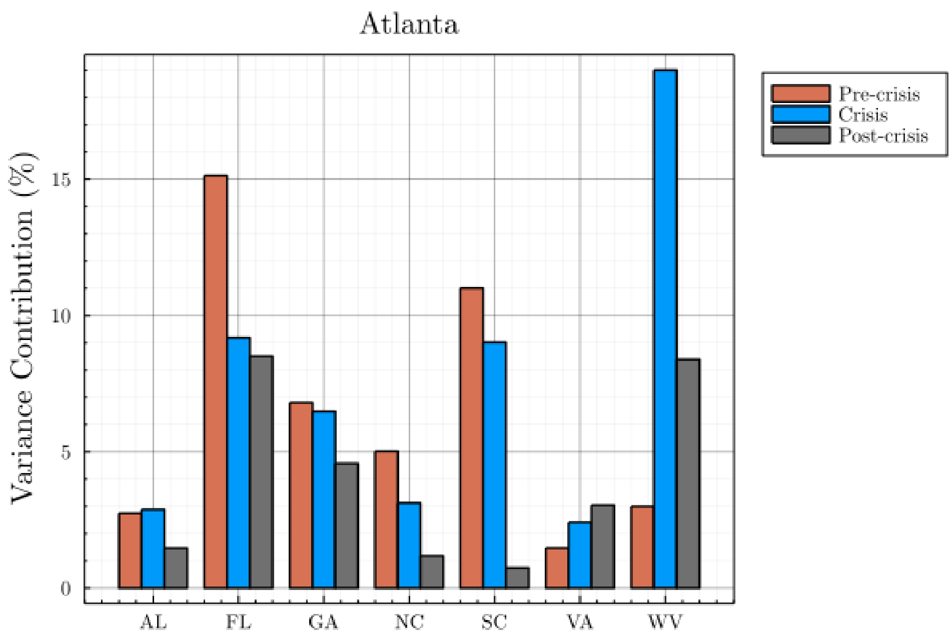

Figure 8: This graph plots the percent variance contribution made by the Atlanta regional factor toward each of the state-average ROE series in the Atlanta region across the pre-, intra-, and post-crisis subsample periods.

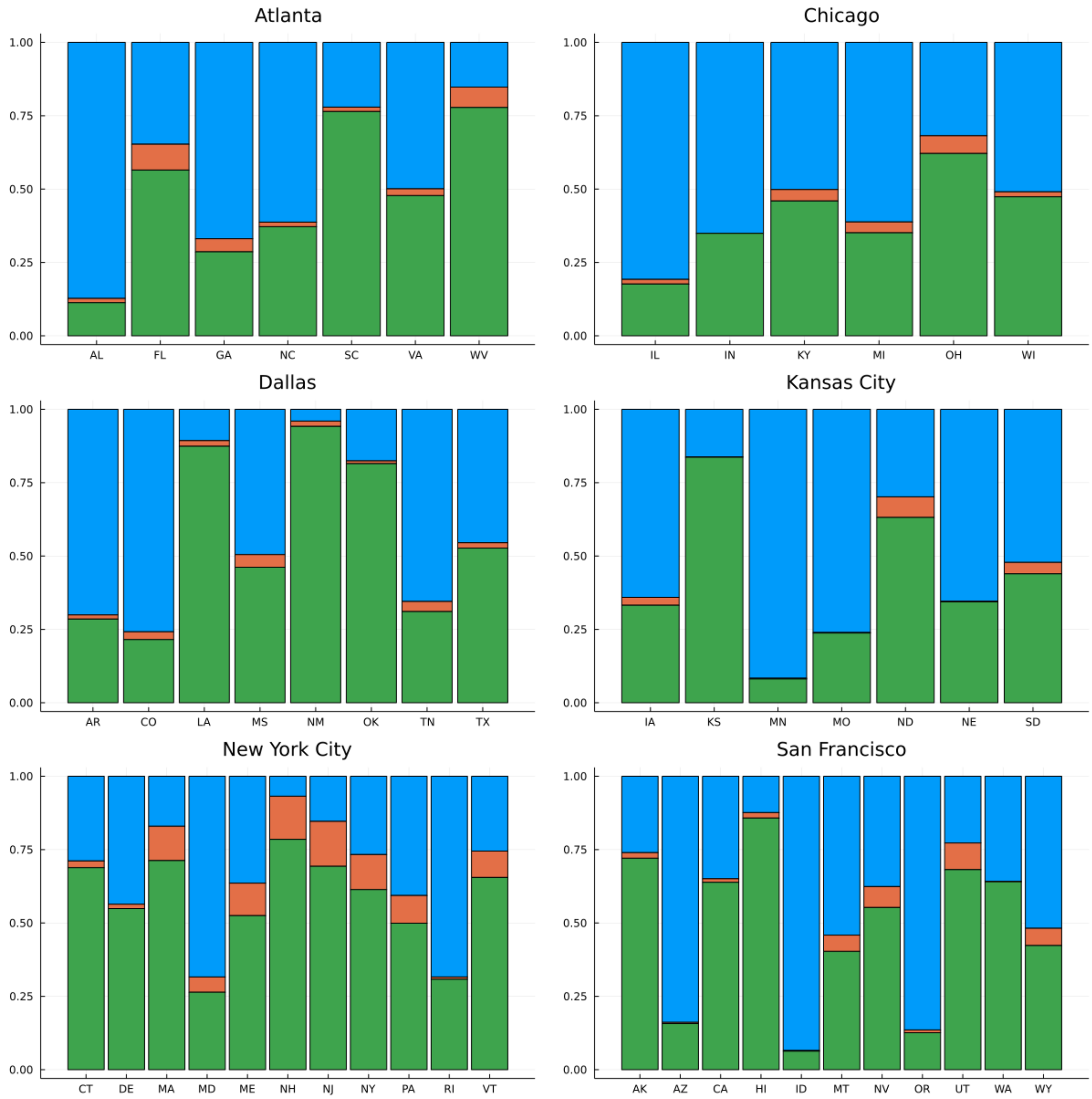

Figure 9: Each of the facets in the given graph presents the variance decomposition of each of the state-average ROE series for a given region with respect to the three non-intercept independent variables: (1) the national factor (in blue), (2) a corresponding regional factor (in orange), and (3) the corresponding state-specific idiosyncratic disturbance process (in green). In other words, the graph shows the percentage of the total variance of each observable series in each region that may be attributed to each of its possible contributing drivers.

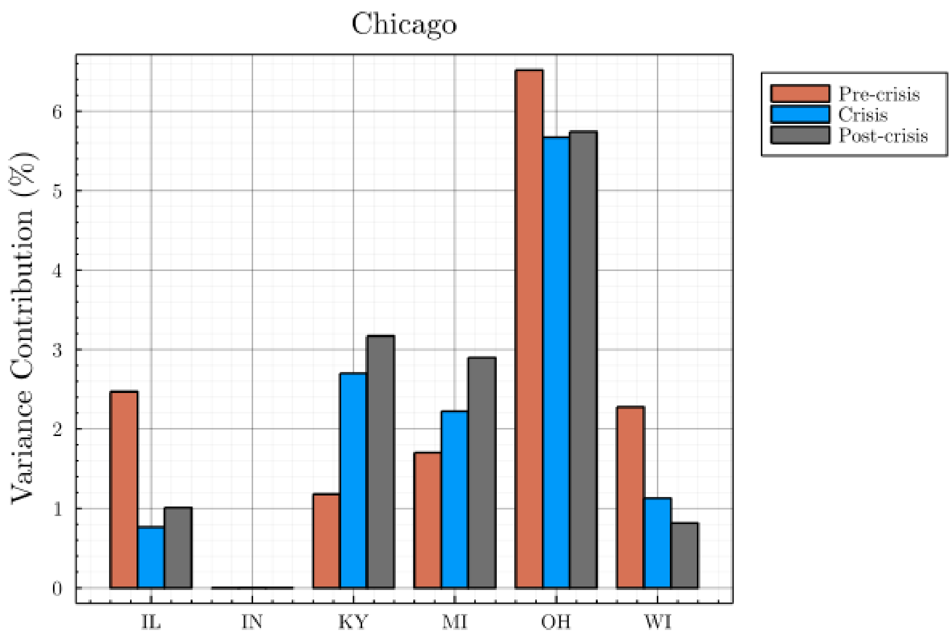

Figure 10: This graph plots the percent variance contribution made by the Chicago regional factor toward each of the state-average ROE series in the Chicago region across the pre-, intra-, and post-crisis subsample periods.

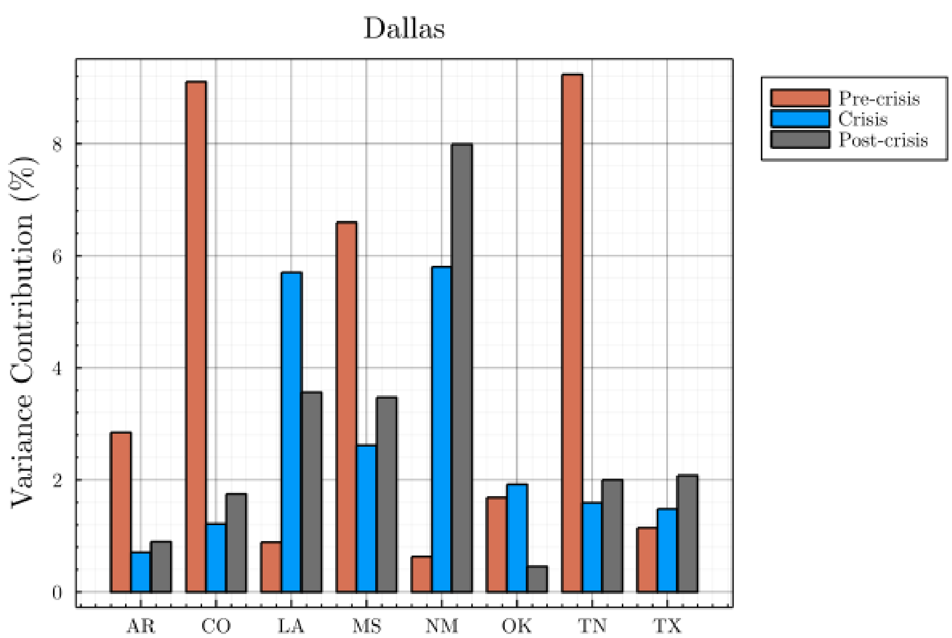

Figure 11: This graph plots the percent variance contribution made by the Dallas regional factor toward each of the state-average ROE series in the Dallas region across the pre-, intra-, and post-crisis subsample periods.

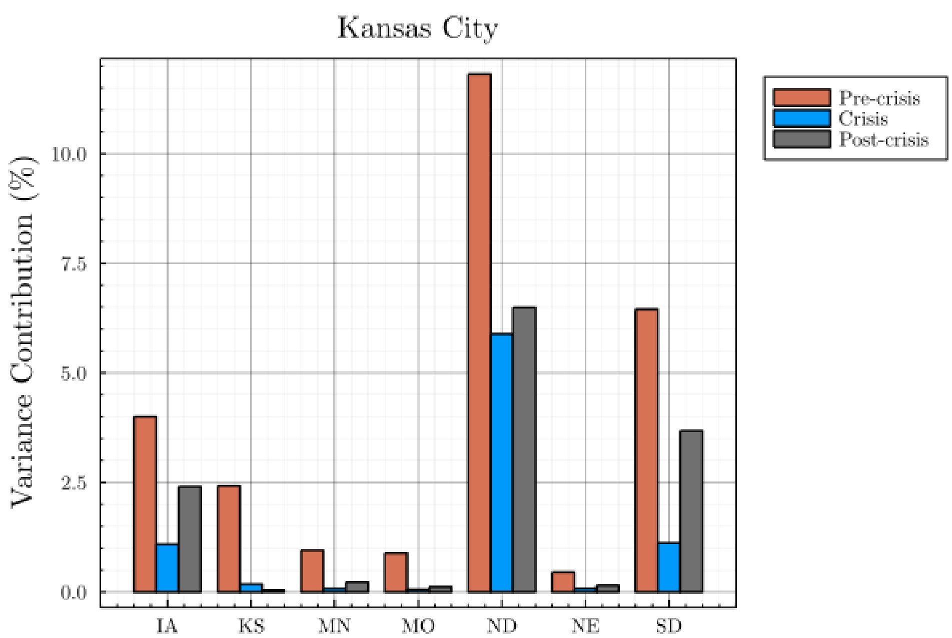

Figure 12: This graph plots the percent variance contribution made by the Kansas City regional factor toward each of the state-average ROE series in the Kansas City region across the pre-, intra-, and post-crisis subsample periods.

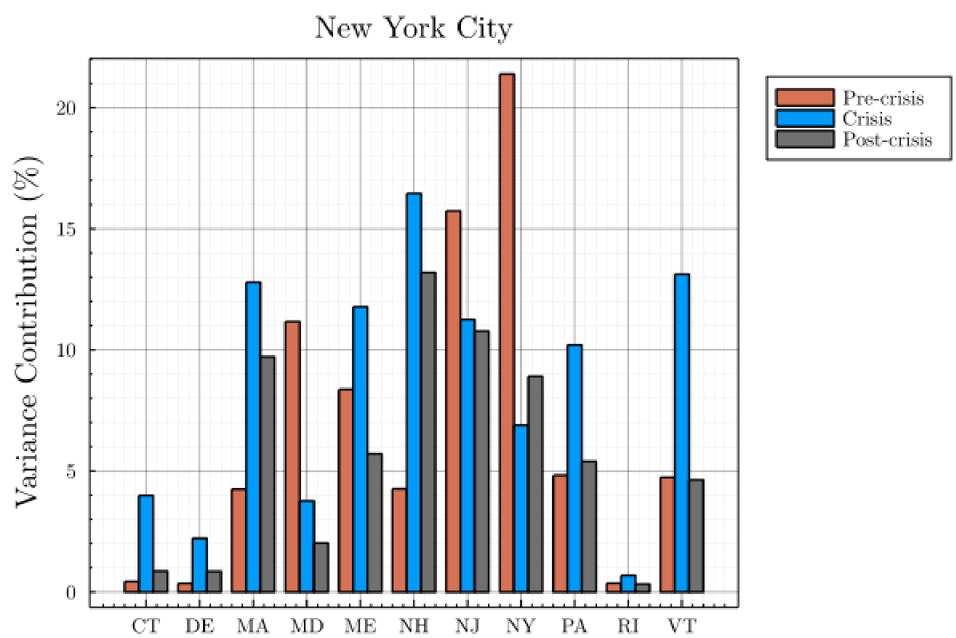

Figure 13: This graph plots the percent variance contribution made by the New York City regional factor toward each of the state-average ROE series in the New York City region across the pre-, intra-, and post-crisis subsample periods.

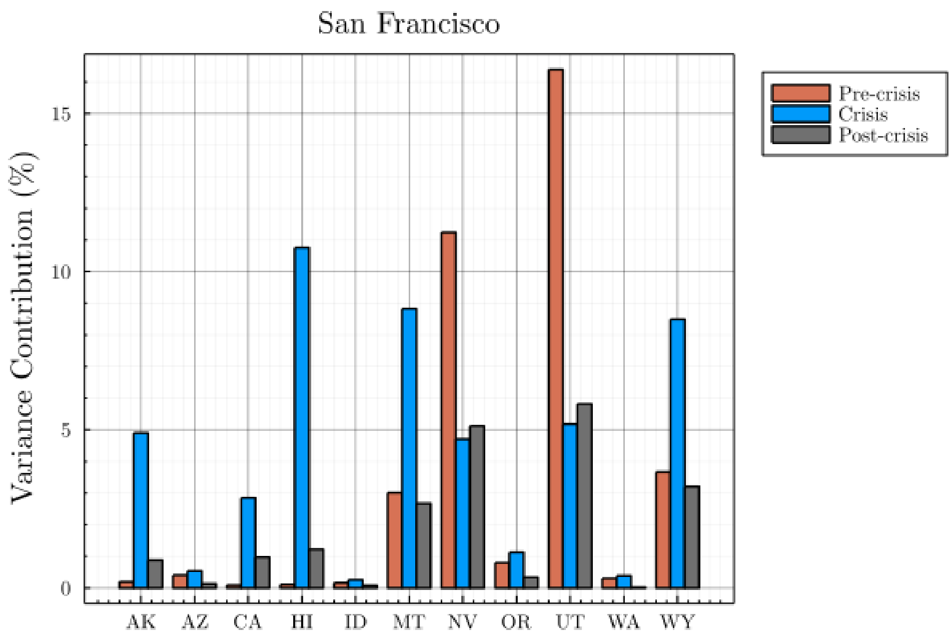

Figure 14: This graph plots the percent variance contribution made by the San Francisco regional factor toward each of the state-average ROE series in the San Francisco region across the pre-, intra-, and post-crisis subsample periods.

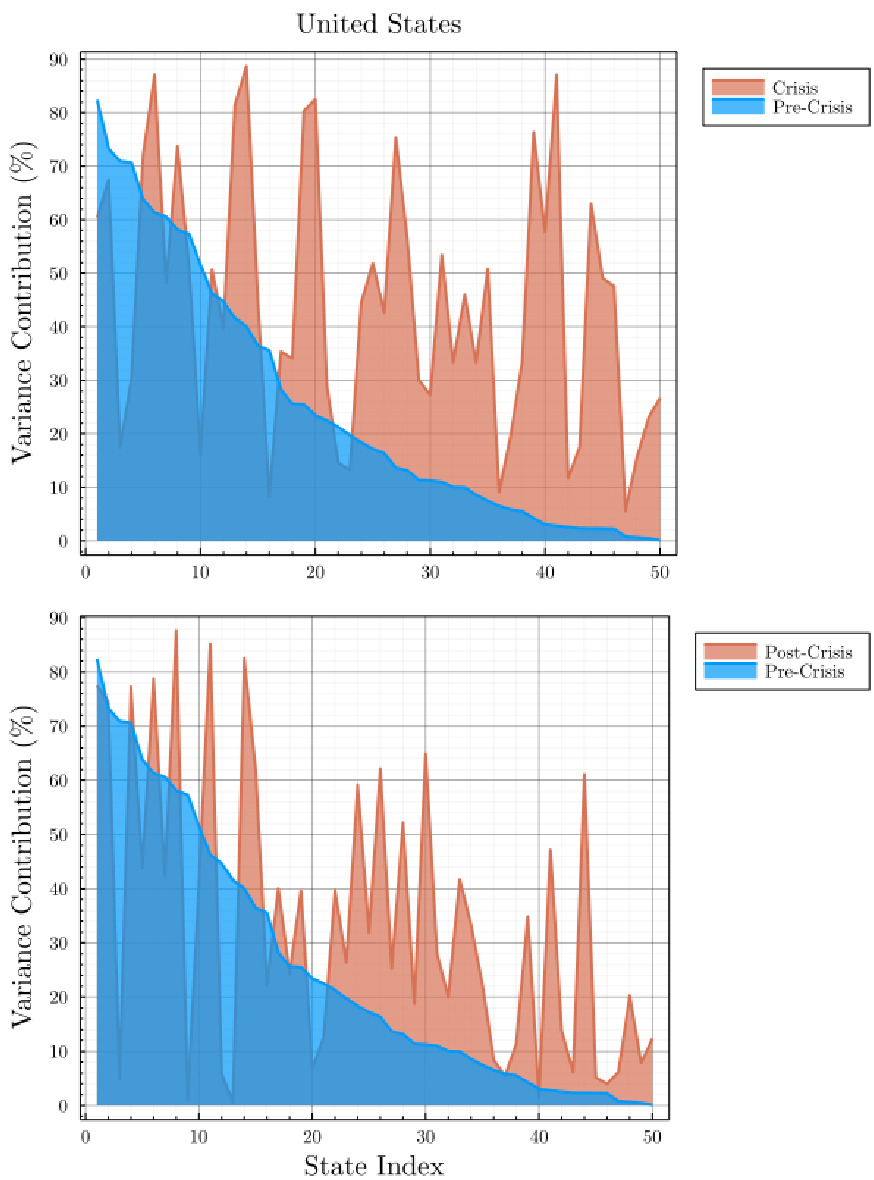

Figure 15: This graph plots the percent variance contribution made by the US national factor toward each of the state-average ROE series in the dataset. In other words, the graph shows the percentage of the total variance of each observable series that may be attributed to the US national factor. The first facet compares the variance contributions made by the national factor during the pre- vs. intra-crisis periods, while the second facet compares that of pre- vs. post-crisis periods. The state index orders states by their pre-crisis national factor contribution in decreasing order.

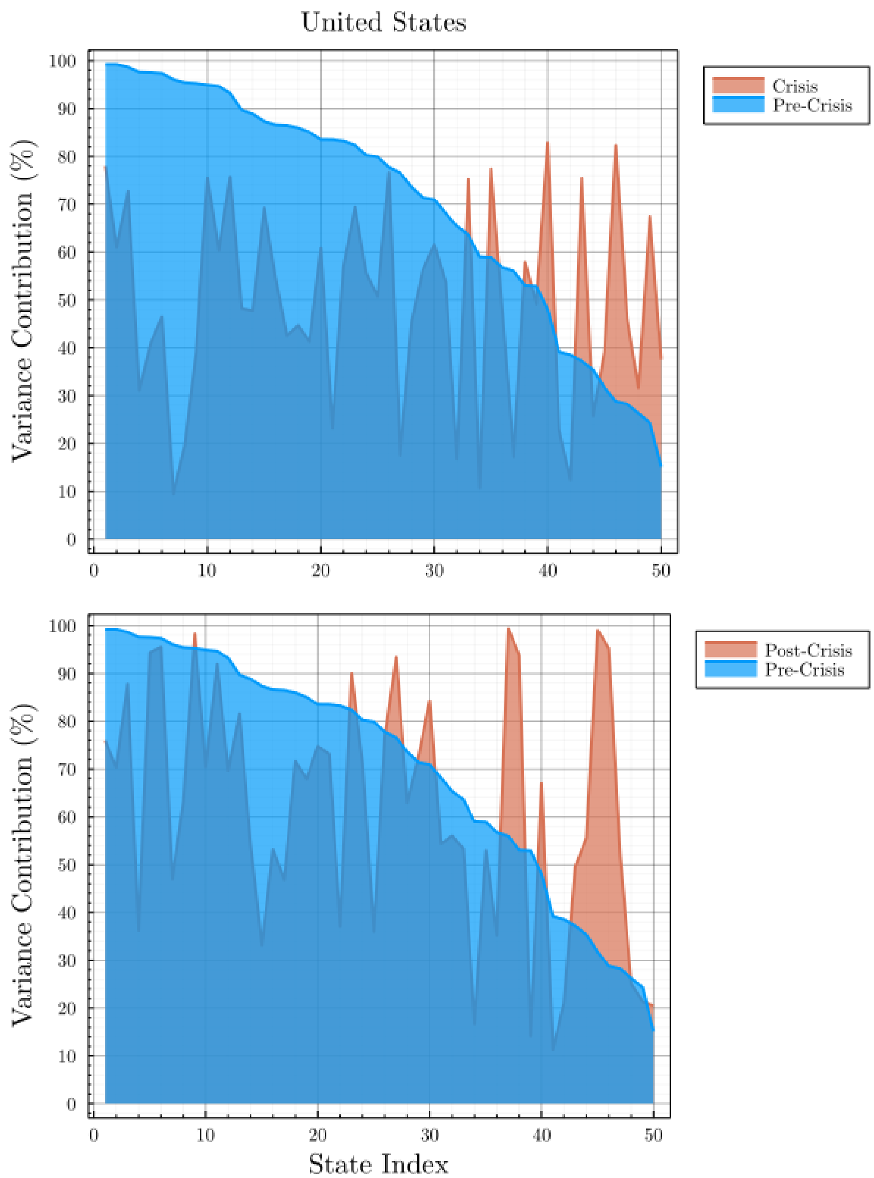

Figure 16: This graph plots the percent variance contribution made toward each of the state-average ROE series in the dataset by their respective idiosyncratic disturbance processes. In other words, the graph shows the percentage of the total variance of each observable series that may be attributed to their corresponding idiosyncratic disturbance processes. The first facet compares the variance contributions during the pre- vs. intra-crisis periods, while the second facet compares that of pre- vs. post-crisis periods. The state index orders states by their pre-crisis national factor contribution in decreasing order.